Potent block of Cx36 and Cx50 gap junction channels by mefloquine

Scott J. Cruikshank*, Matthew Hopperstad†, Meg Younger†, Barry W. Connors*, David C. Spray†, and Miduturu Srinivas†‡

†Department of Neuroscience, Albert Einstein College of Medicine, Bronx, NY 10461; and *Department of Neuroscience, Brown University, Providence, RI 02912

Recently, great interest has been shown in understanding the functional roles of specific gap junction proteins (connexins) in brain, lens, retina, and elsewhere. Some progress has been made by studying knockout mice with targeted connexin deletions. For example, such studies have implicated the gap junction protein Cx36 in synchronizing rhythmic activity of neurons in several brain regions. Although knockout strategies are informative, they can be problematic, because compensatory changes sometimes occur during development. Therefore, it would be extremely useful to have pharmacological agents that block specific connexins, without major effects on other gap junctions or membrane channels. We show that mefloquine, an antimalarial drug, is one such agent. It blocked Cx36 channels, expressed in transfected N2A neuroblastoma cells, at low concentrations (IC$_{50}$ ≈ 300 nM). Mefloquine also blocked channels formed by the lens gap junction protein, Cx50 (IC$_{50}$ ≈ 1.1 μM). However, other gap junctions (e.g., Cx43, Cx32, and Cx26) were only affected at concentrations 10- to 100-fold higher. To further examine the utility and specificity of this compound, we characterized its effects in acute brain slices. Mefloquine, at 25 μM, blocked gap junctional coupling between interneurons in neocortical slices, with minimal nonspecific actions. At this concentration, the only major side effect was an increase in spontaneous synaptic activity. Mefloquine (25 μM) caused no significant change in *evoked* excitatory or inhibitory postsynaptic potentials, and intrinsic cellular properties were also mostly unaffected. Thus, mefloquine is expected to be a useful tool to study the functional roles of Cx36 and Cx50.

Intercellular communication mediated by gap junction channels plays an important role in a variety of tissues, including the nervous system, lens, and heart, by allowing the passage of ions and small molecules between adjacent cells. Gap junction channels are composed of a family of proteins known as connexins (1). Recent studies on connexin-deficient mice and on both humans and rodents harboring dysfunctional connexin mutations have suggested functional roles for some of these proteins (2, 3). For example, mice lacking Cx36, which is primarily expressed in neurons of the brain and retina, exhibit visual disturbances (4) and deficits in synchronous firing within cortical, thalamic, and brainstem circuits (5–7). Mice lacking a major lens connexin, Cx50, have smaller lenses as a result of growth abnormalities and develop cataracts in adulthood (8, 9). In addition to their roles in normal tissue function, gap junctions may also be deleterious in pathological situations such as ischemia by providing a pathway for spread of cellular injury (10) and may communicate cell death to bystanders during development (11). Given the probable importance of gap junction channels in both physiological and pathophysiological situations, it will be desirable to identify drugs that block gap junction channels of specific connexin types while sparing other membrane channels.

Most agents currently being used to block gap junctions, such as *n*-alkanols, volatile anesthetics, and flufenamic acid derivatives, alter many other cellular processes (12, 13). In addition, none of these compounds discriminates between different types of connexins. We recently demonstrated that the antimalarial drug quinine selectively blocks junctions formed by Cx36 and Cx50, without significant effect on several other connexins (i.e., Cx43, Cx26, Cx32, and Cx40) (14). However, because quinine is known to affect a number of voltage- and ligand-gated channels (15, 16), it is of limited utility. In a search for more potent compounds that block certain connexin subtypes without affecting other ion channels, we determined the effect of several derivatives of quinine on gap junction channels and identified mefloquine as one such compound.

Methods

Drugs. Most drugs were obtained from Sigma and were dissolved in external solution as 10 mM stock solutions. Mefloquine was provided by the Drug Synthesis and Chemistry Branch, National Cancer Institute; it was dissolved in DMSO to give 100 mM stock solution and was stored at room temperature.

Junctional Current Measurements in Transfected Cells. Junctional currents were measured on N2A cells either stably transfected with connexins or transiently cotransfected with connexin and enhanced green fluorescent protein cDNAs in separate vectors (14). Each cell of a pair was initially held at 0 mV. Thereafter, 200-msec hyperpolarizing pulses (to −10 mV) were applied to one cell to establish a transjunctional voltage gradient (V_j) and junctional current (I_j) was measured in the second cell. Connexins used were rCx26, rCx32, rCx36, rCx43, rCx46, and mCx50 (where r and m refer to rat and mouse cDNAs). Bathing solution contained 140 mM NaCl, 5 mM KCl, 2 mM CaCl$_2$, 1 mM MgCl$_2$, 5 mM Hepes, 5 mM dextrose, 2 mM pyruvate, 2 mM CsCl, and 1 mM BaCl$_2$ (pH 7.4). Patch electrode resistances were 3–5 MΩ when filled with solution containing 130 mM CsCl, 10 mM EGTA, 0.5 mM CaCl$_2$, and 10 mM Hepes (pH 7.2). Drugs were applied by gravity-fed perfusion. Solution exchanges were complete within 30 sec.

Synaptic Response Measurements from Hippocampal Slices. Transverse hippocampal slices (400 μm thickness) were prepared from 3- to 4-week-old Sprague–Dawley rats. Slices were kept at room temperature for ≥1.5 h before transfer to the recording chamber. Bathing solution (ACSF) contained 124 mM NaCl, 2.5 mM KCl, 10 mM glucose, 25 mM NaHCO$_3$, 1.25 mM NaH$_2$PO$_4$, 2.5 mM CaCl$_2$, and 1.3 mM MgCl$_2$ saturated with 95% O$_2$ and 5% CO$_2$ (pH 7.4). Field excitatory postsynaptic potentials (fEPSPs) were recorded from stratum *radiatum* at room temperature by using patch pipettes filled with 1 M NaCl.

Synaptic Transmission and Coupling in Neocortical Slices. Thalamo-cortical slices (300–400 μm thick) were obtained from rats aged P13–P16 (17). Slices were incubated at 32°C for 45 min, then held at 32°C during recordings. The bath contained 126 mM NaCl, 3 mM KCl, 1.25 mM NaH_2PO_4, 2 mM $MgSO_4$, 26 mM $NaHCO_3$, 10 mM dextrose, and 2 mM $CaCl_2$, saturated with 95% O_2/5% CO_2. Patch pipettes contained 130 mM potassium gluconate, 4 mM KCl, 2 mM NaCl, 10 mM Hepes. 0.2 mM EGTA, 4 mM ATP-Mg, 0.3 mM GTP-Tris, 14 mM phosphocreatine-Tris (pH 7.25, 280–285 mOsm). Recordings were made in whole-cell current-clamp mode, with IR-differential interference contrast visualization. To record from electrically coupled pairs of cells, we targeted closely spaced interneurons with large somata (<100 μm separation) in middle layers of barrel cortex. Two common interneuron classes were identified, based on their action potential shapes and patterns: the fast spiking (FS) and low-threshold spiking cells. We observed electrical coupling mainly among cells within the same class (17, 18). Coupling was measured by injecting negative current pulses (-100 to -400 pA) into one cell of a pair and recording the voltage responses in both cells of the pair. Coupling coefficient was calculated as the response amplitude in the noninjected cell divided by the amplitude in the injected cell. Chemical inhibitory postsynaptic potentials (IPSPs) and their short-term dynamics were also tested. Trains of four action potentials were evoked in a presynaptic cell at 40 Hz while recording associated IPSPs in a monosynaptically connected postsynaptic cell; dynamics were assayed as the ratio of final IPSP amplitude relative to initial IPSP amplitude.

Magnitude of blockade caused by the drugs is expressed as fraction of the control response in the presence vs. absence of the drug, "% control." In general, group results are presented as mean ± SEM.

Results

To initially identify compounds that are more potent than quinine, we determined effects of several derivatives of quinine on Cx50 gap junction currents (Fig. 1). Of these, mefloquine was found to be most potent (see Fig. 1*A* for chemical structures of quinine and mefloquine). Chloroquine (1 mM), amodiaquine (100 μM), and quinacrine (1 mM) produced no significant inhibition of junctional currents (all decreases <12%). Pamaquine caused a greater reduction (30 ± 3% at 1 mM) but still was not nearly as potent as mefloquine (Fig. 1*B*). We therefore characterized mefloquine further, beginning with its potency and specificity for various connexins. We previously found that quinine blocked Cx36 and Cx50 gap junctions with IC_{50} values of 32 and 73 μM, respectively (14), with only moderate effects on other connexins. To determine whether mefloquine had similar specificity, the effect of the drug on channels formed by Cx26, Cx32, Cx36, Cx40, Cx43, Cx46, and Cx50 was tested (Fig. 2). For Cx36, 0.3 and 1 μM mefloquine reduced gap junction channel currents (I_j) by ≈55% and ≈90% (Fig. 2*A*). Recordings from two different cell pairs are illustrated for the two concentrations, because washout of the drug resulted in virtually no recovery of Cx36-mediated currents. The effect on Cx50 was also quite potent, with 3 μM mefloquine reducing I_j by 97% (Fig. 2*B*; see Fig. 2*D* for lower concentrations). Some recovery of I_j on washout of the drug did occur for Cx50, but it was slow and usually incomplete (Fig. 2*B*; mean recovery was 39 ± 7% of initial current, $n = 14$). For Cx43 channels, exposure to 3 μM mefloquine was ineffective in reducing I_j, but complete block could be produced by a 10-fold higher concentration (Fig. 2 *C* and *E*). Reversibility was more complete for Cx43 channels than for more sensitive connexins (Fig. 2*C*; mean recovery was 69 ± 8% of initial current, $n = 8$). Concentration dependence of mefloquine on Cx36 and Cx50 junctional currents is illustrated in Fig. 2*D*. IC_{50} values for mefloquine-induced block were
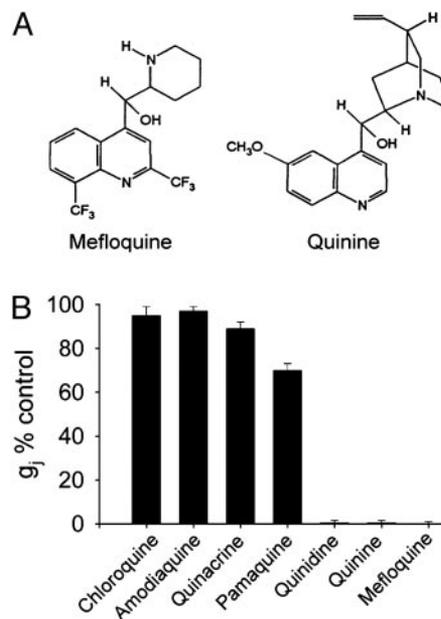
**Fig. 1.** Effect of various analogs of quinine on Cx50 channels. (*A*) Chemical structures of mefloquine and quinine. (*B*) Bar graph summarizing effect of chloroquine (1 mM), amodiaquine (100 μM), quinacrine (1 mM), pamaquine (1 mM), quinidine (stereoisomer of quinine, 300 μM), quinine (300 μM), and mefloquine (100 μM) on Cx50 junctional conductance (g_j) in N2A cells. Each bar represents the mean of four to six cell pairs for each treatment.

interpolated to be 300–400 nM for Cx36 and 1–2 μM for Cx50. Thus, mefloquine is even more potent than quinine on Cx36 and Cx50 channels.

Furthermore, mefloquine was found to be relatively selective for certain connexin subtypes. At concentrations sufficient to cause complete block of Cx36 and Cx50 junctions (e.g., 3 μM), mefloquine had no effect on Cx26, Cx32, Cx43, and Cx46 (data not shown). The effect of 10 and 30 μM on channels formed by different connexins are summarized in Fig. 2*E*. Note that 10 μM mefloquine caused only a small (<10%) reduction in junctional currents for Cx26, Cx32, or Cx46 expressing cells, but somewhat more significant reduction for Cx43 (43%). At 30 μM, magnitude of blockade for Cx26, Cx32, and Cx43 channels was increased (73–99%) but resulted in only 12% reduction in Cx46 currents. These results clearly indicate that effects of mefloquine are connexin subtype-selective.

Cx36 is highly expressed in the brain (19). Studies on knockout mice indicate that the majority of neural electrical synapses revealed electrophysiologically are composed of Cx36, including those in the neocortex, thalamic reticular nucleus, inferior olive, and possibly hippocampus (5–7, 20–22). To further examine the utility of mefloquine, we determined whether it reduced coupling in brain slices from neocortex. To assess coupling, we recorded from pairs of FS or low-threshold spiking interneurons (see *Methods* and Fig. 3*A*). When 25 μM mefloquine was applied to electrically connected interneurons, coupling was markedly reduced (Fig. 3). This reduction occurred in a time- and concentration-dependent manner (Fig. 3 *B* and *C*). Typically, effects were slow, with maximum blockade occurring >70–100 min after drug application. Reduction of coupling was not due to rundown, because coupling strengths were not significantly changed during long-lasting recordings in the absence of drug (Fig. 3 *B* and *C*). Concentrations of mefloquine required to block coupling in neocortical slices were typically 25-fold higher than those observed from blockade of Cx36 coupling in N2A cells. The magnitude of blockade after ≈1 h of 10, 25, and 50 μM

Cruikshank *et al.*

PHARMACOLOGY
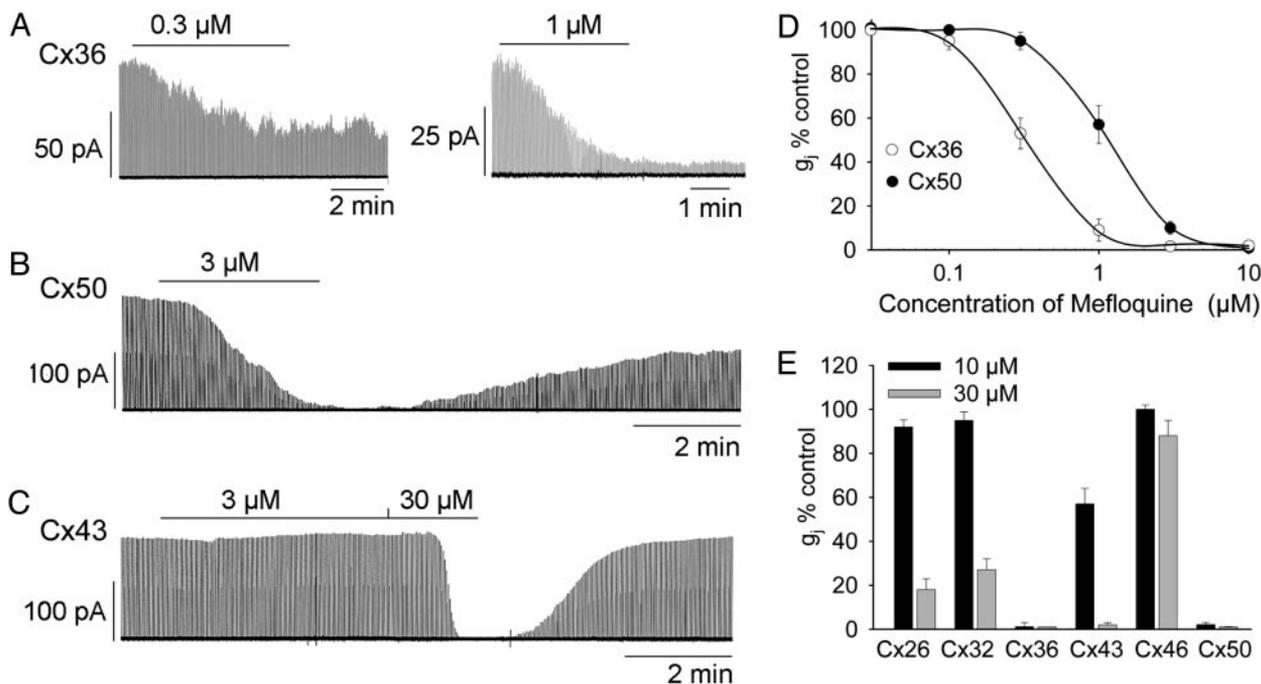
Fig. 2. Mefloquine reduces junctional currents from N2A cells expressing Cx36, Cx50, and Cx43 in a concentration-dependent and connexin-selective manner. (*A*) Mefloquine decreased I_j of Cx36 in a concentration-dependent but irreversible manner. Recordings in *A* are from two separate cell pairs. (*B*) Cx50 channels were almost completely blocked by 3 μM mefloquine. (*C*) Higher concentration was required to elicit closure of Cx43 channels. (*D*) Concentration dependence of mefloquine on Cx36 (○) and Cx50 (●). Each point represents the mean of four to ten cell pairs. Each cell pair was exposed to only a single concentration. (*E*) Effect of 10 and 30 μM mefloquine on Cx26, Cx32, Cx36, Cx43, Cx46, and Cx50. Each bar represents the mean of four to six cell pairs.

mefloquine was 29, 66, and 99%, respectively (Fig. 3*C*; extrapolated IC$_{50}$ $\approx$ 15 μM).

The antimalarial compounds quinine and quinidine block a wide variety of cellular processes, including voltage-gated channels (15, 16). In contrast, relatively little is known of mefloquine's action on other ion channels, although it has been reported to block some voltage- and volume-gated channels (23–26; see below). To determine the relative specificity of mefloquine for gap junction channels over other channels, we studied its effects on chemical synapses and intrinsic cell properties in the hippocampus and neocortex (Figs. 4 and 5). The only major nonspecific effect we observed was an increase in *spontaneous* synaptic activity. An example of this is illustrated in Fig. 4*A* for an FS interneuron exposed to 25 μM mefloquine. Similar effects were observed in 15 of 21 cells. Application of DMSO (the vehicle for the drug) alone for 80–100 min did not cause increases in spontaneous activity, indicating that observed changes were caused by mefloquine (*n* = 3). We further determined whether increases in spontaneous activity produced by mefloquine were caused by glutamate receptor activation by testing the effects of the drug during ionotropic glutamate receptor blockade (2.0–2.4 mM kynurenic acid, bath applied at least 15 min before mefloquine; Fig. 4*B*). Kynurenic acid blocked the vast majority of spontaneous activity in the control condition and prevented any obvious increases during mefloquine application. Similar results occurred in 5 FS cells, suggesting that the mefloquine-induced increase in spontaneous activity is mainly mediated by glutamatergic transmission. Finally, we determined that the increased spontaneous activity was not caused by presynaptic spiking in two ways. First, for 5 FS cells, the addition of 1 μM tetrodotoxin (TTX) to the bath did not block the increase in synaptic activity (Fig. 4*A*). Second, in five regular spiking (RS) cells (i.e., excitatory pyramidal cells), 25 μM mefloquine

produced only moderate depolarization (3.0 $\pm$ 1.1 mV) and no action potentials.

The results above indicate that mefloquine caused clear increases in spontaneously occurring, action potential-independent synaptic activity (i.e., miniature synaptic potentials). However, similar concentrations of the drug had little effect on *evoked* chemical synaptic activity (Fig. 4 *C* and *D*). To examine effects on excitatory transmission, we measured fEPSPs from the CA1 region of the hippocampus before and during application of 10, 30, and 100 μM mefloquine. Application of 10 and 30 μM elicited little change in fEPSP ($\leq$5% decrease), and a significant decrease was achieved only at higher concentrations of 100 μM (44% decrease; Fig. 4*C*).

To test the effect of mefloquine on evoked inhibitory synaptic transmission, we recorded IPSPs from monosynaptically paired interneurons in neocortical slices (Fig. 4*D* and *Methods*). As illustrated in Fig. 4*D*, application of mefloquine (25 and 50 μM) had little effect on IPSP amplitudes (mean changes <10%) or their short-term depression.

To further explore whether mefloquine affects other neuronal properties, we measured the effect of the drug on action potentials from inhibitory interneurons in neocortical slices. Long trains of action potentials were elicited with 600-msec depolarizing steps in control ACSF, then in the presence of 25 μM mefloquine (Fig. 5); a variety of spike parameters were measured. As shown in Fig. 5*B*, mefloquine had little effect on most spike parameters. However, mefloquine did have three minor effects on spiking as illustrated in Fig. 5. First, a modest reduction occurred in spike height at the end of a long train (Fig. 5 *A* and *B*). Second, the drug induced an increase in spike frequency adaptation (Fig. 5 *A* and *C*). Third, mefloquine induced a suppression of delay before spiking in FS cells (Fig. 5*A*, arrow). For each of these effects, we determined whether mefloquine or DMSO was causal by comparing spike trains before and after 80–100 min of perfusion of 12.8 μM DMSO,
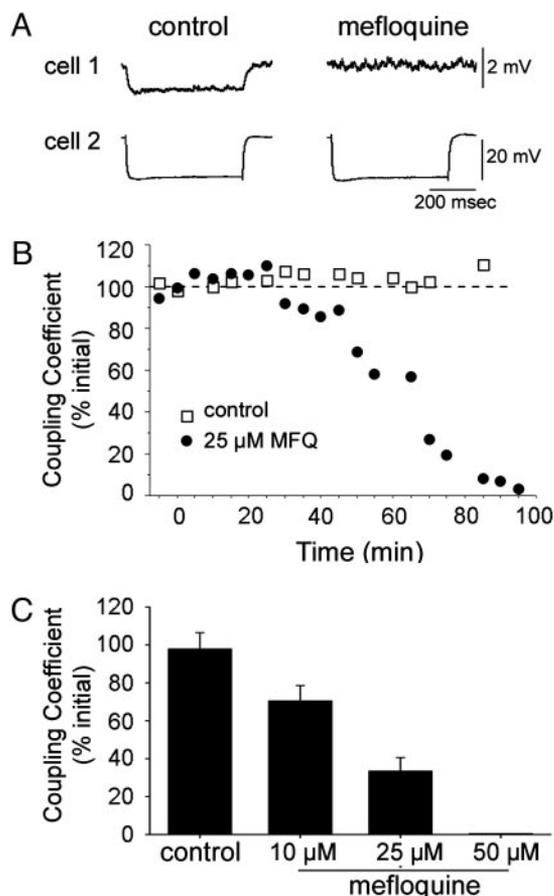
Fig. 3. Mefloquine reduces coupling between interneurons in rat neocortical slices. (*A*) Effect of mefloquine on electrical coupling between a pair of FS interneurons. Test current steps (−400 pA) were applied to cell 2. Illustrated traces are average voltage responses from 15 sequential steps. (*B*) Time course of coupling during perfusion of mefloquine (MFQ) or of normal ACSF (the mefloquine pair is the same as in *A*). Voltage responses in the injected cell and in the electrically coupled cell were measured to estimate the coupling coefficient ($\Delta V_{coupled\ cell}/\Delta V_{injected\ cell}$). Coupling was blocked by mefloquine but not significantly changed during long-lasting recordings in the absence of the drug. (*C*) Group data showing concentration dependence of mefloquine. Magnitude of block was quantified after ≈1 h in the absence and presence of mefloquine. Each bar represents the mean ($n = 4$ pairs, 3 pairs, 5 pairs, and 1 pair for control ACSF, 10 μM, 25 μM, and 50 μM mefloquine, respectively).

which was the concentration used in the mefloquine experiments ($n = 3$ FS cells). Spike properties were unaffected by DMSO ($P > 0.05$), indicating that observed changes were caused by mefloquine.
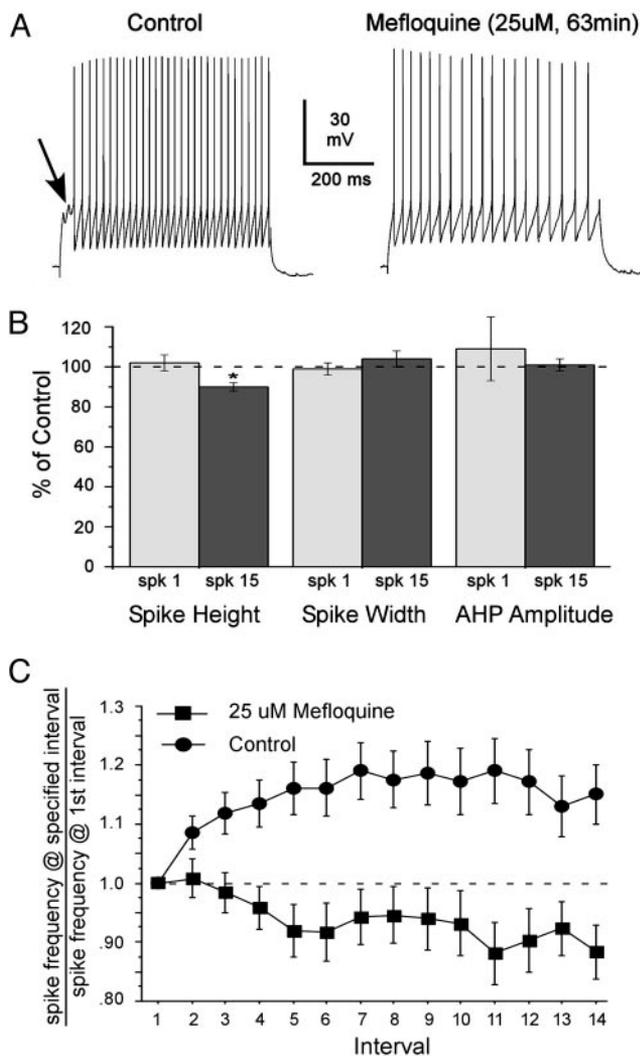
A theoretical study predicts that complete blockade of electrical synapses should approximately double input resistance of cortical interneurons, owing to the large contribution of these synapses to total membrane conductance (27). Although we observed a significant increase in R_{in} (Fig. 6), it averaged <20% above control values ($n = 10$). This failure to observe the larger predicted change in R_{in} may have been due to an offsetting increase in membrane conductance associated with the observed increase in spontaneous glutamatergic activity. To test this, we blocked the increase in spontaneous activity by using kynurenic acid (see above) and then measured the change in R_{in} produced by 25 μM mefloquine. In these cases, R_{in} increased >50% above control values ($n = 5$; Fig. 6), supporting the idea that electrical synapses contribute a large portion of the membrane conductance of neocortical interneurons. Surprisingly, the apparently large conductance produced by glutamate receptor activation
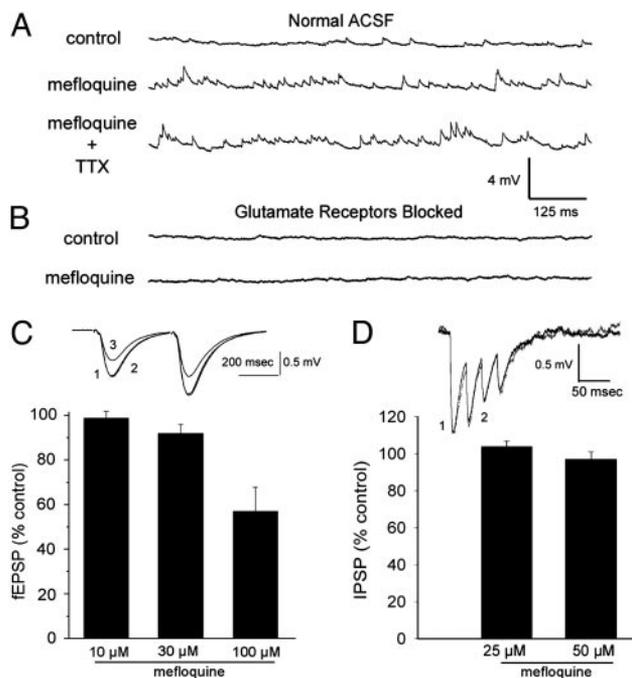
Fig. 4. Effect of mefloquine on spontaneous and evoked chemical synaptic transmission. (*A*) Spontaneous activity recorded from FS interneuron before and 61 min after exposure to 25 μM mefloquine. Spontaneous activity was clearly increased by mefloquine. An additional 20–30 min of application of TTX (1 μM) did not reduce spontaneous activity in this or four other FS cells subjected to TTX. In this group, spontaneous synaptic event frequencies went from 44.2 ± 13.6 Hz during baseline, to 91.8 ± 18.1 Hz in mefloquine, and 104.6 ± 17.3 Hz after 20–30 min of TTX. Event amplitudes were 0.50 ± 0.03 mV, 0.64 ± 0.05 mV, and 0.64 ± 0.05 mV for the baseline, mefloquine, and TTX conditions, respectively. (*B*) Another FS cell recorded during blockade of ionotropic glutamate receptors by kynurenic acid (2.4 mM). Note blockade of spontaneous synaptic activity in both control and mefloquine conditions. (*C*) Effect of mefloquine on fEPSPs recorded from the CA1 area of the hippocampus. Effects were determined for 10 μM (for 60 min; $n = 3$), 30 μM (for 50 min; $n = 3$), and 100 μM (for 30 min; $n = 4$) in different slices. Reduction of evoked activity was observed only at the highest concentration of the drug. Sample traces measured in control ("1") and after application of 30 μM ("2") and 100 μM ("3") mefloquine are superimposed. Note the lack of obvious change in short-term facilitation. (*Bottom*) Group effects on fEPSPs. (*D*) Mefloquine did not affect IPSPs measured from somatosensory cortex. Sample traces taken before ("1") and 80 min after 25 μM mefloquine ("2") are superimposed. Each record is average of 20 traces. The presynaptic cell (an FS interneuron) was injected with short depolarizing steps (5 msec) to induce four action potentials at 40 Hz (one train every 12 sec). The postsynaptic cell (a low-threshold spiking interneuron) was continuously injected with depolarizing current to hold the steady-state membrane potential at about −50 mV, revealing IPSPs as negative deflections. Note that no obvious change occurs in either response amplitude or short-term depression. (*Bottom*) Bar graph showing group effects on IPSPs ($n = 4$ for 25 μM, $n = 2$ for 50 μM).
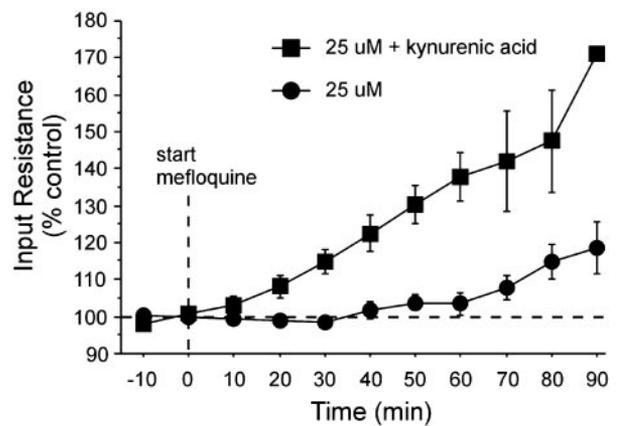
did not result in a correspondingly large depolarization; for five FS cells, membrane potential was allowed to run free, and the average mefloquine-induced depolarization was just 1.2 ± 2.0 mV. Potentially, this lack of depolarization could be caused by offsetting inhibitory conductances, which would not be readily observed as IPSPs at the membrane potentials recorded here (mean V_m in mefloquine was −62.4 ± 2.2 mV). This matter will require further investigation.

The majority of neocortical slice experiments in this study focused on interneurons because they are electrically coupled, whereas excitatory RS cells are not. Nevertheless, we examined a small sample of RS cells ($n = 5$) to further determine possible effects of mefloquine on membrane potential, R_{in}, spike height and width in response to 600-msec steps. None of these prop-

Cruikshank *et al.*

Fig. 6. Mefloquine increases input resistance (R_{in}). R_{in} (as % control) is plotted as a function of mefloquine perfusion duration. Cells bathed in normal ACSF before mefloquine ($n = 10$) are plotted separately from those bathed in ACSF containing kynurenic acid (2.0–2.4 mM; $n = 5$). Note larger increase in R_{in} for the kynurenic acid group.

addition, as with FS cells, mefloquine also increased spontaneous synaptic activity in RS cells.

Discussion

In this study, we identified a pharmacological agent that can be used specifically to study roles of connexins primarily responsible for intercellular communication in the lens (Cx50) and in retinal and CNS neurons and pancreatic islet β cells (Cx36). In N2A cells, mefloquine reduced Cx36 and Cx50 junctional currents with IC_{50} values of 0.31 and 1.1 μM, respectively. Block of Cx36 gap junction channels occurred at concentrations that were 50-fold lower than those observed for the complete inhibition of other connexins expressed in the brain (e.g., Cx43, Cx32, and Cx26). Similarly, mefloquine inhibited Cx50 channels at a 100-fold lower concentration than required for the other lens gap junction protein, Cx46, making it a useful tool to study the role of Cx50 in the lens, although sensitivity of Cx46/Cx50 heteromers and of cleaved forms of Cx50, which are known to be expressed in the lens, remain to be tested (28, 29)

Mefloquine also blocked coupling between interneurons in neocortical slices (Fig. 3). However, this reduction occurred at concentrations 25-fold higher than required to achieve complete blockade in N2A cells. A possible explanation for this large difference could be that concentrations of the drug at the recording site are lower than in bath solution as a result of slow drug diffusion through slices. Mefloquine binds tightly to phospholipid membranes, and thus drug concentrations deep in the slices may be lower than in bath solution. More complete equilibration of the drug would be expected under conditions of chronic antimalarial therapy (during which plasma and brain levels reach 1–6 μM; refs. 30–32), allowing the possibility that side effects of mefloquine administration, such as anxiety, confusion, dizziness, dysphoria, and severe neuropsychiatric effects, might be due to gap junction blockade.

Our studies indicate that concentrations of mefloquine that block coupling between neocortical interneurons exerted only moderate effects on chemical synapses or intrinsic cell properties, suggesting that the drug may be useful to delineate the roles of Cx36 and Cx50 without many of the nonspecific effects associated with other uncoupling agents currently in use. These results are in marked contrast to the effects of quinine, which blocks certain gap junction channels and voltage-gated channels with similar potency. However, it must be noted that mefloquine does have some nonspecific effects. Mefloquine causes increases in spontaneous synaptic activity and affects spiking during long high-

Fig. 5. Effect of mefloquine on spiking in interneurons of rat neocortex. (*A*) Representative spike trains from control and 25 μM mefloquine conditions for an FS cell. The trains are matched for initial spike rate. Three main effects of mefloquine on spiking are illustrated. First, notice the slight decrease in spike amplitude across the train for the mefloquine condition but not the control. Second, note the increase in spike frequency adaptation in mefloquine, such that the later intervals in the train become longer. Third, although a characteristic delay occurs in spiking after the initial depolarization during the control period (see arrow), no such delay occurs in mefloquine. Drug-induced reductions in delays before onset of spiking occurred in 6 of 9 FS cells that showed delays in the control condition. (*B*) Group effects of mefloquine on three spike parameters for early and late spikes in trains (mean % control, $n = 14$ cells). Spike width and AHP amplitude were not affected, nor was height of the first spike in trains. A modest but significant decrease in height occurred for spikes late within trains (15th spike; $P < 0.05$, mefloquine vs. control, paired *t* test). (*C*) Group results on spike frequency adaptation. Spike frequency for each interspike interval is plotted as fraction of the frequency during the initial interval; thus, values >1.0 indicate increased frequency compared with the first interval, whereas values <1 indicate decreased frequencies. Note that frequencies increase during the train in control conditions but decrease in mefloquine. Differences between the two conditions are significant for all intervals after the second ($P < 0.05$, $n = 11$ FS cells).

erties changed >15% after 70 min of mefloquine perfusion (25 μM). However, the effect on R_{in}, although small, was statistically significant (mean increase, 13.9 ± 4.8%, $P = 0.046$, paired *t* test). Because RS cells are not electrically coupled, this effect is likely due to a nonspecific action of the drug, tempering any coupling-related interpretation of R_{in} changes in the interneurons. In

Cruikshank *et al.*

frequency trains (Figs. 4 and 5). Previous studies also indicate nonspecific actions: mefloquine has been shown to block L-type calcium channels and delayed rectifier channels in cardiac myocytes, volume- and calcium-activated chloride channels, and ATP-sensitive potassium channels. IC_{50} values for blockade of these channels in single, dissociated cells, a situation similar to our studies on N2A cells, are 3- to 15-fold higher than those required for Cx36 blockade (23–26). Because of these effects, use of mefloquine to study roles of Cx36 and Cx50 should be accompanied by proper controls.

Mefloquine was nearly 75-fold more potent at blocking Cx36 and Cx50 gap junctions than was quinine. We believe that this large difference in potency arises from substitutions in the quinoline ring and/or in the aliphatic ring structure. In comparison with quinine, which contains an acetyl group on the quinoline ring, mefloquine contains two —CF_3 groups on this aromatic ring. This modification significantly enhances the lipophilicity of the drug. In addition, the quinucludine ring in quinine is replaced in mefloquine by a piperidine ring. Compounds that lack the aliphatic ring structure, such as chloroquine, did not block gap junction channels. Structure–activity studies should lead to better understanding of the regions of the molecule that are important for block and also allow identification of potent and more specific analogs of mefloquine that

block not only Cx36 and Cx50, but also other connexins expressed at high levels in the heart and brain (e.g., Cx43).

Conclusions

Recent studies on knockout mice indicate that expression of Cx36 is essential for coupling in various regions of the brain and for transmission of rod signals in the retina (4–7, 19–22). Similarly, Cx50 expression has been demonstrated to be essential for lens growth, development, and maintenance of transparency (8). However, reliance on knockout mice to exclusively delineate the roles of connexins is problematic. For example, Cx36-deficient mice have a number of morphological and electrophysiological changes besides the lack of this connexin, and gene-profiling experiments in Cx43 null astrocytes reveal alterations in a large number of genes with diverse functions (33, 34). Thus, a pharmacological agent such as mefloquine that inhibits Cx36 and Cx50 channels with minimal side effects will be extremely useful for establishing the physiological roles of these connexin subtypes and for verifying changes in phenotype in connexin-deficient mice.

1. Willecke, K., Eiberger, J., Degen, J., Eckardt, D., Romualdi, A., Guldenagel, M., Deutsch, U. & Sohl G. (2002) *Biol. Chem.* **383,** 725–737.
2. White, T.W. & Paul, D. L. (1999) *Annu. Rev. Physiol.* **61,** 283–310.
3. Guldenagel, M., Ammermuller. J., Feigenspan, A., Teubner, B., Degen, J., Sohl, G., Willecke, K. & Weiler, R. (2001) *J. Neurosci.* **21,** 6036–6044.
4. Deans, M. R., Volgyi, B., Goodenough, D. A., Bloomfield, S. A. & Paul, D. L. (2002) *Neuron* **36,** 703–712.
5. Deans, M. R., Gibson, J. R., Sellitto, C., Connors, B. W. & Paul, D. L. (2001) *Neuron* **31,** 477–485.
6. Hormuzdi, S. G., Pais, I., LeBeau, F. E., Towers, S. K., Rozov, A., Buhl, E. H., Whittington, M. A. & Monyer, H. (2001) *Neuron* **31,** 487–495.
7. Landisman, C. E., Long, M. A., Beierlein, M., Deans, M. R., Paul, D. L. & Connors, B. W. (2002) *J. Neurosci.* **22,** 1002–1009.
8. White T. W., Goodenough, D. A. & Paul, D. L. (1998) *J. Cell. Biol.* **143,** 815–825.
9. White, T.W. (2002) *Science* **295,** 319–320.
10. Lin, J. H., Weigel, H., Cotrina, M. L., Liu, S., Bueno, E., Hansen, A. J., Hansen, T. W., Goldman, S. & Nedergaard, M. (1998) *Nat. Neurosci.* **1,** 494–500.
11. Cusato, K., Bosco, A., Rozental, R., Guimaraes, C. A., Reese, B. E., Linden, R. & Spray, D. C. (2003) *J. Neurosci.* **23,** 6413–6422.
12. Spray, D. C., Rozental, R. & Srinivas, M. (2002) *Curr. Drug. Targets* **3,** 455–464.
13. Rouach, N., Segal, M., Koulakoff, A., Giaume, C. & Avignone, E. (2003) *J. Physiol. (London)* **553,** 729–745.
14. Srinivas, M., Hopperstad, M. G. & Spray, D. C. (2001) *Proc. Natl. Acad. Sci. USA* **98,** 10942–10947.
15. Yatani, A., Wakamori, M., Mikala, G. & Bahinski, A. (1993) *Circ. Res.* **73,** 351–359.
16. Snyders, J., Knoth, K. M., Roberds, S. L. & Tamkun, M. M. (1992) *Mol. Pharmacol.* **41,** 322–330.
17. Gibson, J. R., Beierlein, M. & Connors, B. W. (1999) *Nature* **402,** 75–79.
18. Galarreta, M. & Hestrin, S. (1999) *Nature* **402,** 72–75.
19. Rash, J. E., Staines, W. A., Yasumura, T., Patel, D., Furman, C. S., Stelmack, G. L. & Nagy, J. I. (2000) *Proc. Natl. Acad. Sci. USA* **97,** 7573–7538.
20. Long, M. A., Deans, M. R., Paul, D. L. & Connors, B. W. (2002) *J. Neurosci.* **22,** 10898–10905.
21. Buhl, D. L., Harris, K. D., Hormuzdi, S. G., Monyer, H. & Buzsaki, G. (2003) *J. Neurosci.* **23,** 1013–1018.
22. Maier, N., Guldenagel, M., Sohl, G., Siegmund, H., Willecke, K. & Draguhn, A. (2002) *J Physiol.* **541,** 521–528.
23. Kang, J., Chen, X. L., Wang, L. & Rampe, D. (2001) *J. Pharmacol. Exp. Ther.* **299,** 290–296.
24. Gribble, F. M., Davis, T. M., Higham, C. E., Clark, A. & Ashcroft, F. M. (2000) *Br. J. Pharmacol.* **131,** 756–760.
25. Maertens, C., Wei, L., Droogmans, G. & Nilius, B. (2000) *J. Pharmacol. Exp. Ther.* **295,** 29–36.
26. Coker, S. J., Batey, A. J., Lightbown, I. D., Diaz, M. E. & Eisner, D. A. (2000) *Br. J. Pharmacol.* **129,** 323–330.
27. Amitai, Y., Gibson, J. R., Beierlein, M., Patrick, S. L., Ho, A. M., Connors, B. W. & Golomb, D. (2002) *J. Neurosci.* **22,** 4142–4152.
28. Kistler, J. & Bullivant, S. (1987) *Invest. Ophthalmol. Visual Sci.* **28,** 1687–1692.
29. Jiang, J. X. & Goodenough, D. A. (1996) *Proc. Natl. Acad. Sci. USA* **93,** 1287–1291.
30. Karbwang, J. & White, N. J. (1990) *Clin. Pharmacokinet.* **19,** 264–279.
31. Foley, M. & Tilley, L. (1998) *Pharmacol. Ther.* **79,** 55–87.
32. Palmer, K. J., Holliday, S. M. & Brogden, R. N. (1993) *Drugs* **52,** 430–475.
33. De Zeeuw, C. I., Chorev, E., Devor, A., Manor, Y., Van Der Giessen, R. S., De Jeu, M. T., Hoogenraad, C. C., Bijman, J., Ruigrok, T. J., French, P., et al. (2003) *J. Neurosci.* **23,** 4700–4711.
34. Iacobas, D. A., Urban, M., Iacobas, S., Scemes, E. & Spray, D. C. (2003) *Physiol. Genom.* **15,** 177–190.

PHARMACOLOGY